

# OpenStereo: A Comprehensive Benchmark for Stereo Matching and Strong Baseline

Xianda Guo<sup>1</sup>, Juntao Lu<sup>1\*</sup>, Chenming Zhang<sup>1\*</sup>, Yiqi Wang<sup>1</sup>, Yiqun Duan<sup>1</sup>,  
Tian Yang<sup>2</sup>, Zheng Zhu<sup>2</sup>, and Long Chen<sup>1,3†</sup>

<sup>1</sup> Waytous  
<sup>2</sup> GigaAI

<sup>3</sup> Institute of Automation, Chinese Academy of Sciences  
xianda\_guo@163.com, long.chen@ia.ac.cn

**Abstract.** Stereo matching aims to estimate the disparity between matching pixels in a stereo image pair, which is of great importance to robotics, autonomous driving, and other computer vision tasks. Despite the development of numerous impressive methods in recent years, replicating their results and determining the most suitable architecture for practical application remains challenging. Addressing this gap, our paper introduces a comprehensive benchmark focusing on practical applicability rather than solely on performance enhancement. Specifically, we develop a flexible and efficient stereo matching codebase, called **OpenStereo**. OpenStereo includes training and inference codes of more than 10 network models, making it, to our knowledge, the most complete stereo matching toolbox available. Based on OpenStereo, we conducted experiments and have achieved or surpassed the performance metrics reported in the original paper. Additionally, we carry out an exhaustive analysis and deconstruction of recent developments in stereo matching through comprehensive ablative experiments. These investigations inspired the creation of StereoBase, a strong baseline model. Our StereoBase ranks 1<sup>st</sup> on SceneFlow, KITTI 2015, 2012 (Reflective) among published methods and achieves the best performance across all metrics. In addition, StereoBase has strong cross-dataset generalization. Code is available at <https://github.com/XiandaGuo/OpenStereo>.

## 1 Introduction

Stereo matching is a fundamental topic in the field of computer vision, aiming to compute the disparity between a pair of rectified stereo images. It plays a crucial role in numerous applications such as robotics [60], autonomous driving [30, 39], and augmented reality [53], as it enables depth perception and 3D reconstruction of the observed scene.

---

\* Joint second authors.

† Corresponding authors

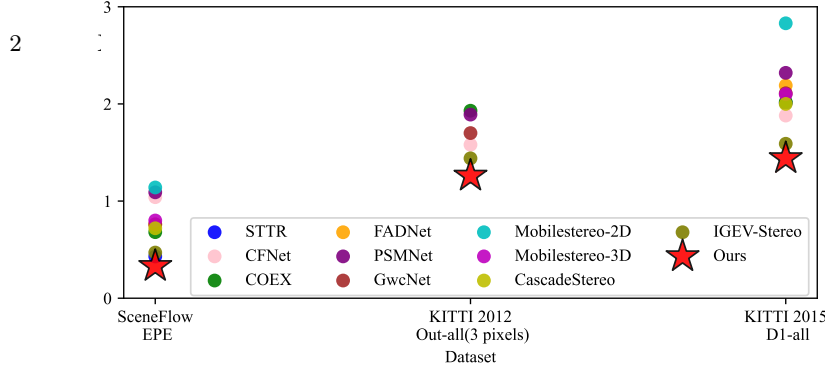


**Fig. 1:** Comparison with other state-of-the-art stereo methods [1, 5, 12, 13, 24, 39, 40, 46, 51] on SceneFlow [28], KITTI 2012 [11], 2015 [29] leaderboards.

Traditional stereo matching algorithms typically rely on matching corresponding image regions between the left and right views based on their similarity measures. Several techniques have been proposed in the literature for stereo matching, including methods based on gray-level information [2, 23, 56], region-based approaches [33, 62], and energy optimization methods [16, 37]. Gray-level-based methods [2, 23, 56] compute disparities by matching pixels or groups of pixels with similar intensities in the left and right images. Region-based approaches [33, 62] group pixels into larger regions and then compute correspondences between these regions. Energy optimization methods [16, 37] formulate the stereo matching problem as an energy minimization problem, where the goal is to find the disparity map that minimizes a certain energy function. While these methods have achieved some success in stereo matching, they suffer from certain limitations and challenges, such as occlusions, textureless regions, and computational complexity.

Recently, with the support of large synthetic datasets [11, 28, 29, 36, 38], CNNs-based stereo matching methods [5, 7, 13, 19, 25, 46, 52, 58] has achieved impressive results. These methods have shown remarkable performance in terms of accuracy and efficiency. Unlike traditional methods, CNN-based stereo matching methods are end-to-end frameworks that take a pair of stereo images as input and directly predict the disparity between them. In addition to the accuracy and efficiency benefits, CNN-based stereo matching methods have shown the potential for generalization to new environments and scenes beyond the training data. This is mainly due to the ability of CNNs to learn feature representations from raw data that are invariant to scale, rotation, and illumination changes. Furthermore, the availability of large-scale datasets has enabled the use of deep learning techniques for stereo matching, allowing for more complex and sophisticated models to be trained.

Nevertheless, we find that not all datasets are accompanied by official evaluation tools. For example, the DrivingStereo [55] dataset does not provide specific evaluation scripts, making comparative assessments challenging. The SceneFlow [28] dataset, with its finalpass and cleampass data varieties, complicates fair model comparisons. Generalization experiments for stereo matching algorithms typically train on the SceneFlow dataset and evaluate on KITTI2012 [11], KITTI2015 [29], ETH3D [38], and Middlebury [36]. However, the inconsistency in evaluation data volume and metric definitions across studies leads to compara-

tive discrepancies. Furthermore, even when source codes for models are available, reproducing the reported benchmarks is exceedingly challenging, *e.g.* STTR [24]. Hence, there's a pressing need for a comprehensive benchmark study within the stereo matching community to enhance practicality and ensure consistent comparisons. To achieve this objective, we introduce a versatile stereo matching codebase: OpenStereo.

To promote scalability and adaptability, OpenStereo offers the following features: (1) **Modual design**, researchers can define a new model without the need to alter the model code itself by simply modifying a yaml configuration file. (2) **Various frameworks**, including Concatenation-based [5, 58], Correlation-based [1, 45, 46, 52], Interlaced-based [39], Group-wise-correlation-based [51], Combine-based methods [13], and Difference-based [21]. (3) **Various datasets**, including SceneFlow [28], KITTI2012 [11], KITTI2015 [29], Middlebury [36], ETH3D [38] and DrivingStereo [55] dataset. (4) **State-of-the-art methods**, including PSMNet [5], GwcNet [13], AANet [52], FADNet++ [46], CFNet [40], STTR [24], CoEx [1], CascadeStereo [12], MobileStereoNet [39] and IGEV [51].

Leveraging OpenStereo, we rigorously reassess various officially stated conclusions by meticulously re-implementing the ablation studies, including data augmentation, backbone architectures, cost construction, disparity regression and refinement processes. Based on the insights gleaned from these ablation experiments, we introduce StereoBase, a model that sets a new benchmark, surpassing recently proposed methods in terms of performance. Furthermore, we undertake a thorough investigation to establish that StereoBase is not only powerful but also serves as an empirically robust baseline model for stereo matching, demonstrating exceptional efficacy and resilience across diverse testing scenarios.

In summary, this paper makes significant contributions to the field of stereo matching research from three key aspects. (1) **OpenStereo**, a unified and extensible platform, enables researchers to conduct comprehensive stereo matching studies. (2) With the support of OpenStereo, we conduct a profound revisit and thorough deconstruction of recent stereo matching methodologies. (3) We introduce **StereoBase**, which sets a new benchmark with EPE of 0.34 on SceneFlow [28] and ranks 1<sup>st</sup> on KITTI2015 [29] and 2012(Reflective) [11] leaderboards among published methods. Furthermore, StereoBase exhibits exceptional cross-dataset generalization capabilities. These contributions collectively advance the state-of-the-art in stereo matching, offering both insights and practical tools to the stereo matching research community.

## 2 Related Work

### 2.1 Stereo Matching

With the rapid development of CNNs, significant progress has been made in stereo matching. Based on the network pipeline of stereo matching, stereo matching methods can be roughly grouped into two categories [46], including

the encoder-decoder network with 2D convolution (ED-Conv2D) and the cost volume matching with 3D convolution (CVM-Conv3D).

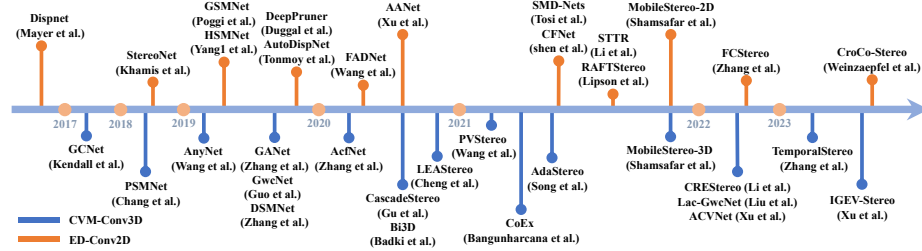


**Fig. 2:** Timeline of Stereo Matching Models. This figure illustrates the timeline of various stereo matching models that have been proposed in the literature. The top part shows ED-conv2D-based models, while the bottom part shows CVM-conv3D-based models. Each model is labeled with its name and authors.

**Stereo Matching with CVM-Conv3D** The CVM-Conv3D methods are proposed to improve the performance of depth estimation [1, 5, 7, 12, 13, 19, 22, 26, 31, 39, 41, 44, 50, 58, 59]. These methods learn disparities from a 4D cost volume, which is mainly constructed by concatenating left feature maps with their corresponding right counterparts across each disparity level [5]. GCNet [19] firstly introduced a novel approach that combines 3D encoder-decoder architecture with a 2D convolutional network to obtain a dense feature representation, which is used to regularize a 4D concatenation volume. Following GCNet [19], PSMNet [5] proposes an approach for regularizing the concatenation volume by leveraging a stacked hourglass 3D convolutional neural network in tandem with intermediate supervision. In order to enhance the expressiveness of the cost volume and ultimately improve performance in ambiguous regions, GwcNet [58] proposes the group-wise correlation volume and ACVNet [50] proposes the attention concatenation volume. GANet [58] proposes a semi-global aggregation layer and local guided aggregation layer to capture local and the whole-image cost dependencies respectively. Based on GANet [58], DSMNet [59] construct a robust “domain normalization” method to overcome the challenges in cross-domain generalization. CoEx [1] proposes a novel approach called Guided Cost volume Excitation (GCE), which leverages image guidance to construct a simple channel excitation of the cost volume. IGEV-Stereo [51] leverages an iterative geometry encoding volume to capture both local and non-local geometry information, which outperforms existing methods on KITTI benchmarks and achieves cross-dataset generalization and high inference efficiency. Besides, as a potential solution to reduce the need for humans to design a good volumetric method, Neural Architecture Search (NAS) [3, 15, 27] has been employed in stereo matching [7].

However, these CVM-Conv3D methods still suffer from low time efficiency and high memory requirements, which are far from real-time inference even on

server GPUs. Therefore, it is essential to address the accuracy and efficiency problems for real-world applications.

**Stereo Matching with ED-Conv2D** The ED-Conv2D methods [9, 21, 24, 25, 28, 34, 35, 39, 40, 43, 46, 52, 54, 57, 61], which adopt networks with 2D convolutions to predict disparity, has been driven by the need for improved accuracy, computational efficiency, and real-time performance. One of the early deep learning-based stereo matching methods, MC-CNN (Matching Cost CNN) [57], was proposed to learn a matching cost function for improving performance in the cost aggregation and optimization stages. Subsequently, Mayer *et al.* [28] present end-to-end networks for the estimation of disparity, called DispNet, which is pure 2D CNN architectures. However, the model still faces challenges in capturing the matching features, resulting in poor estimation results. To overcome this challenge, the correlation layer is introduced in the end-to-end architecture [8, 17, 18, 28] to better capture the relationship between the left and right images. By incorporating this layer, the accuracy of the model is significantly improved. Furthermore, FAD-Net++ [46] proposes an innovative approach to efficient disparity refinement using residual learning [14] in a coarse-to-fine manner. AutoDispNet [35] applied neural architecture search to automatically design stereo matching network structures. More recently, Croco-Stereo [47] shows that large-scale pre-training can be successful for stereo matching through well-adapted pretext tasks. This method can achieve state-of-the-art performance without using task-specific designs, like correlation volume or iterative estimation.

These works represent the significant progress that has been made in the field of stereo matching, highlighting the diverse range of methods and architectures that have been proposed to address the challenges associated with this problem.

## 2.2 Codebase

Numerous infrastructure code platforms have been developed in the deep learning research community, with the aim of facilitating research in specific fields. One such platform is OpenGait [10], a gait recognition library. OpenGait thoroughly examines the latest advancements in gait recognition, providing novel perspectives for subsequent research in this domain. In object detection, MMDection [6] and Detectron2 [49] have emerged as an all-encompassing resource for several favored detection techniques. In pose estimation, OpenPose [4] has developed the first open-source system that operates in real-time for detecting the 2D pose of multiple individuals, including the detection of key points for the body, feet, hands, and face. In stereo matching, it is noteworthy that not all datasets are accompanied by official evaluation tools. For instance, the DrivingStereo [55] dataset does not have official evaluation codes, and there is a lack of unified tools for assessing the model generalization across different domains. This absence of standardized evaluation resources contributes to the observed discrepancies in cross-domain evaluations of the same model as reported in different studies. Therefore, it is time to build a benchmark for stereo matching.

### 3 OpenStereo

In recent years, there has been a proliferation of new frameworks and evaluation datasets for stereo matching. However, the lack of a unified and fair evaluation platform in this field is a significant issue that cannot be ignored. To address this challenge and promote academic research and practical application we have developed **OpenStereo**, a pyTorch-based [32] toolbox that provides a reliable and standardized evaluation framework for stereo matching.

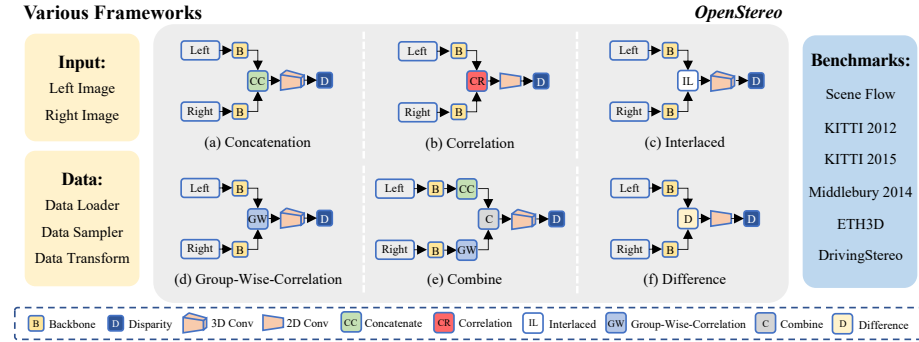


**Fig. 3:** The design principles of proposed codebase OpenStereo.

#### 3.1 Design Principles of OpenStereo

As shown in Figure 3, our developed OpenStereo covers the following highlight features.

**Modular Design.** OpenStereo adopts a modular design, greatly facilitating researchers in exploring new networks. By simply modifying a YAML configuration file, researchers can define a new model without the need to alter the model code itself. This design significantly lowers the barriers for researchers to extend or integrate additional algorithms and modules within the framework. This approach empowers researchers to freely combine and customize their algorithms with minimal code composition, enhancing the framework’s usability and adaptability.

**Compatibility with various frameworks.** Currently, more and more stereo matching methods have emerged, such as Concatenation-based [5, 7, 19, 58], Correlation-based [1, 45, 46, 52], Group-wise-correlation-based [51], Difference-based [21], Interlaced-based [39], and Combine-based methods [13, 40]. As mentioned above, many open-source methods have a narrow focus on their specific models, making it challenging to extend to multiple frameworks. However, OpenStereo provides a solution to this problem by supporting all of the aforementioned frameworks. With OpenStereo, researchers and practitioners can easily compare and evaluate different stereo matching models under a standardized evaluation protocol.

**Support for various evaluation datasets.** OpenStereo is a comprehensive tool that includes datasets commonly used by researchers in stereo matching. OpenStereo not only supports synthetic stereo datasets such as SceneFlow [28], but also five real-world datasets: KITTI2012 [11], KITTI2015 [29], ETH3D [38], Middlebury [36], and DrivingStereo [55]. We introduce a suite of bespoke functions, meticulously crafted for each dataset, encompassing everything from initial data preprocessing to the final stages of evaluation. The evaluation module includes the submission of the results to all benchmarks.

**Support for state-of-the-arts.** In our work, we have successfully replicated various state-of-the-art stereo matching methods, including PSMNet [5], GwcNet [13], AANet [52], FADNet++ [46], CFNet [40], STTR [24], CoEx [1], CascadeStereo [12], MobileStereoNet [39] and IGEV [51]. Notably, the performance metrics we achieved, in most cases, surpass those reported in their original publications. This comprehensive replication effort provides a valuable resource for novices in the field, offering a rich array of official examples to facilitate an effective and efficient start in stereo matching research.

### 3.2 Main Modules

Technically, we follow the design of most PyTorch deep learning projects and divide OpenStereo into three modules, *data*, *modeling*, and *evaluation*.

*Data module* includes three key components: data loader, which is responsible for loading and preprocessing the data; data sampler, which is used to select a subset of data for each iteration; and data transform, which applies various transformations to the data to increase the diversity and complexity of the training set.

*Modeling module* is built upon the `BaseModel` base class, which predefines many behaviors of the stereo matching during both training and testing phases. This module consists of four essential components, namely the *Feature Extraction*, *Cost Calculation*, *Cost Aggregation*, and *Disparity Processor*, which are critical to current stereo matching algorithms.

*Evaluation module* is utilized to assess the performance of the obtained model. Recognizing that different datasets require distinct evaluation protocols, we have incorporated these varied protocols directly into OpenStereo, significantly simplifying the evaluation process.

## 4 Revisit Deep Stereo Matching

### 4.1 Recheck on Previous Methods

PSMNet [5] is one of the most crucial and frequently cited networks in stereo matching. The official implementation code is available at <https://github.com/pytorch/vision>. GwcNet [13] employs a Group-wise Correlation Stereo Network to exploit both local and global matching cost volumes (<https://github.com/xy-guo/GwcNet>). AANet [52] focuses on adaptively fusing multi-scale features through a lightweight and efficient adaptive aggregation module (

<https://github.com/haofeixu/aanet>). FADNet++ [46] employs a two-stage architecture, consisting of a feature-metric aggregation stage and a disparity refinement stage. (<https://github.com/HKBU-HPML/FADNet>). CFNet [40] utilizes a collaborative feature learning strategy to enhance the representation capacity of features in the matching cost computation (<https://github.com/gallensz1/CFNet>). STTR [24] focuses on geometric correspondence problems, including stereo matching, by employing transformers to capture long-range spatial and temporal context information (<https://github.com/ml0603/stereo-transformer>). CoEx [1] focuses on context-aware features and cost volume aggregation (<https://github.com/antabangun/coex>). CascadeStereo [12] adopts a cascaded architecture for accurate and efficient disparity estimation, whose official code is available at (<https://github.com/alibaba/cascade-stereo>). MobileStereoNet [39] builds upon the StereoNet [21], which proposes Interlacing Cost Volume Construction (<https://github.com/cogsys-tuebingen/mobilestereonet>). IGEV [51] builds a combined geometry encoding volume that not only encodes both geometric and contextual information but also intricately captures fine-grained details of local matching (<https://github.com/gangweiX/IGEV>).

**Table 1:** Quantitative evaluation on the SceneFlow [28] test. For each model, the specific category on the SceneFlow used is consistent with the original paper. Models marked with  $\dagger$  are OpenStereo implementations, others are from the original paper. Underline refers to evaluation in the non-occluded regions only [24]. Bold: Best

| Method                         | SceneFlow        |            |             |
|--------------------------------|------------------|------------|-------------|
|                                | TrainSize        | Categories | EPE(px)     |
| STTR [24]                      | 256 $\times$ 512 | FinalPass  | 0.43        |
| STTR [24] $\dagger$            | 256 $\times$ 512 | FinalPass  | 0.40        |
| PSMNet [5]                     | 256 $\times$ 512 | CleanPass  | 1.09        |
| PSMNet [5] $\dagger$           | 256 $\times$ 512 | CleanPass  | <b>0.96</b> |
| CFNet [40]                     | 256 $\times$ 512 | FinalPass  | 1.04        |
| CFNet [40] $\dagger$           | 256 $\times$ 512 | FinalPass  | <b>0.96</b> |
| AA-Net [52]                    | 288 $\times$ 576 | CleanPass  | 0.87        |
| AA-Net [52] $\dagger$          | 288 $\times$ 576 | CleanPass  | <b>0.80</b> |
| Mobilestereo-2D [39]           | 256 $\times$ 512 | FinalPass  | 1.14        |
| Mobilestereo-2D [39] $\dagger$ | 256 $\times$ 512 | FinalPass  | <b>1.10</b> |
| Mobilestereo-3D [39]           | 256 $\times$ 512 | FinalPass  | 0.80        |
| Mobilestereo-3D [39] $\dagger$ | 256 $\times$ 512 | FinalPass  | <b>0.79</b> |
| GwcNet [13]                    | 256 $\times$ 512 | FinalPass  | 0.76        |
| GwcNet [13] $\dagger$          | 256 $\times$ 512 | FinalPass  | <b>0.74</b> |
| COEX [1]                       | 288 $\times$ 576 | FinalPass  | 0.68        |
| COEX [1] $\dagger$             | 288 $\times$ 576 | FinalPass  | <b>0.67</b> |
| FADNet++ [46]                  | 384 $\times$ 768 | CleanPass  | 0.76        |
| FADNet++ [46] $\dagger$        | 384 $\times$ 768 | CleanPass  | <b>0.65</b> |
| CascadeStereo [12]             | 256 $\times$ 512 | FinalPass  | 0.72        |
| CascadeStereo [12] $\dagger$   | 256 $\times$ 512 | FinalPass  | <b>0.67</b> |
| IGEV [51]                      | 320 $\times$ 736 | FinalPass  | 0.47        |
| IGEV [51] $\dagger$            | 320 $\times$ 736 | FinalPass  | <b>0.46</b> |

**Table 2:** Quantitative evaluation on KITTI2015 leadboard.

| Method                  | KITTI2015   |             |             |
|-------------------------|-------------|-------------|-------------|
|                         | D1-bg       | D1-fg       | D1-all      |
| PSMNet [5]              | 1.86        | 4.62        | 2.32        |
| PSMNet [5] <sup>†</sup> | <b>1.80</b> | <b>4.58</b> | <b>2.26</b> |
| IGEV [51]               | <b>1.38</b> | 2.67        | <b>1.59</b> |
| IGEV [51] <sup>†</sup>  | 1.44        | <b>2.31</b> | <b>1.59</b> |

For benchmarking, it is critical to ensure that the results are reliable and trustworthy. To achieve this, we conducted our experiments using SceneFlow [28] and KITTI2015 [29] datasets. As shown in Table 1, in most cases, the reproduced performances of OpenStereo are better than the results reported by the original papers. Regarding the KITTI2015 dataset, submission constraints led us to limit our leaderboard contributions to reproductions of the widely recognized PSM-Net [5] and the latest state-of-the-art IGEV [51], as demonstrated in Table 2. We stand by the integrity of our benchmark, asserting its role in providing a reliable and valid evaluation of stereo matching models. OpenStereo is designed to offer the research community in stereo matching a standardized, comprehensive platform for method assessment. This facility enables meaningful and comparative analyses across various models, thereby serving as an valuable tool for the innovation and scrutiny of emerging algorithms.

## 4.2 Denoising Stereo Matching

With the support of OpenStereo, a comprehensive reevaluation of various stereo matching methods is conducted, including data augmentation, feature extraction, cost construction, disparity prediction and refinement.

**Table 3:** The model undergoes training and evaluation on the finalpass of the SceneFlow [28] training and test sets. KITTI2015 [29] training set, consisting of 200 images, is only employed to evaluate the generalizability of models under various data augmentation conditions. RC stands for RandomCrop. CES represents ColorAug, Erase, and Scale. HFlip denotes both images of a stereo and disparity are horizontally flipped. HSFlip horizontally flips both images in the stereo pair and then swaps them. VFlip involves vertically flipping both images in the stereo pair along with the disparity, inverting their top-bottom orientation. <sup>†</sup> denotes the method proposed in this paper.

| Data Augmentation                  | SceneFlow<br>EPE(px) | KITTI15     |             |
|------------------------------------|----------------------|-------------|-------------|
|                                    |                      | EPE(px)     | D1_all      |
| RC(256×512)                        | 0.5856               | 3.13        | 17.61       |
| RC(320×736)                        | 0.5632               | 1.75        | 8.97        |
| BatchRandom <sup>†</sup>           | 0.5688               | 2.78        | 13.20       |
| RC(320×736)+HFlip                  | 0.5955               | 2.84        | 13.05       |
| RC(320×736)+HSflip                 | 0.8706               | 2.35        | 17.02       |
| RC(320×736)+Vflip                  | 0.5629               | 2.24        | 12.87       |
| RC(320×736)+ColorAug               | 0.5861               | <b>1.61</b> | <b>7.81</b> |
| RC(320×736)+Scale                  | 0.6895               | 2.70        | 15.76       |
| RC(320×736)+Shift(10) <sup>†</sup> | 0.5702               | 2.66        | 14.95       |
| RC(320×736)+Erase                  | <b>0.5606</b>        | 2.83        | 15.03       |
| RC(320×736)+CE                     | 0.5831               | 1.66        | 7.97        |
| RC(320×736)+CES                    | 0.7132               | 1.75        | 8.97        |

**Data Augmentation** While five data augmentation techniques are prevalent in stereo matching [25, 51], including random crop, color augmentation, eraser transform, flip, and spatial transform, the empirical efficacy of each method specifically for stereo vision tasks remains an underexplored area in the field. Our work extends beyond these common practices, exploring not only these techniques but also experimenting with two additional methods: BatchRandom and Shift, to further understand their impact on stereo matching performance. BatchRandom denotes the technique applied during model training where the size of the random crop varies for each batch. The Shift involves randomly shifting the right image horizontally by a certain range and then cropping both images to a specified size. As shown in Table 3, most data augmentation strategies, except for the combined use of erase transform and random crop, lead to a decline in the model’s performance metrics of SceneFlow. This is because stereo matching involves pixel-level matching, and these data augmentations (color augmentation, flip, and spatial transform) can affect the alignment of pixels. The erase transform benefits stereo matching by enhancing the model’s capacity to cope with occlusions, missing data, and diverse real-world scenarios. It encourages robust feature learning and generalization, ultimately improving model performance. Furthermore, the combination of RandomCrop( $320 \times 736$ ) with color augmentation delivers the most striking improvements in Kitti2015 dataset performance, achieving the lowest EPE of 1.61 px and the lowest D1\_all of 7.81. Such improvements highlight the critical role of color augmentation in boosting the model’s resilience against the variability of color and lighting that naturally occurs in diverse driving environments.

**Table 4:** Ablation study of different backbones and pre-training methods on the final-pass of SceneFlow test datasets [28]. Flops and Params represent the computational complexity and parameters within the whole model, respectively.

| Backbone              | Pre-train | Flops   | Params | EPE           |
|-----------------------|-----------|---------|--------|---------------|
| FadNet++ [46]         | None      | 28.39G  | 1.77M  | 0.8633        |
| MobileNetV2 100 [51]  | None      | 31.83G  | 2.78M  | 0.8227        |
| PSMNet [5]            | None      | 130.87G | 4.46M  | 0.8068        |
| MobileNetV2 100 [51]  | None      | 31.83G  | 2.78M  | 0.8227        |
| MobileNetV2 100 [51]  | Timm [48] | 31.83G  | 2.78M  | 0.7132        |
| MobileNetV2 120d [51] | Timm [48] | 38.75G  | 5.21M  | <b>0.6603</b> |

**Feature Extraction** In Table 4, we delve into an ablation study to examine the impact of different backbones and pre-training methods. Initially, we evaluate different backbones without any pre-training. The backbone of FadNet++ [46], despite its low parameter count of 1.77M, results in an EPE of 0.8633, indicating less precision in disparity estimation. Employing MobileNetV2 100 [51] as a backbone improves the EPE to 0.8227, with a slight increase in computational demand (31.83G flops) and parameters (2.78M). The backbone of PSMNet [5], while the most computationally intensive (130.87G flops) with the highest number of parameters (4.46M), achieves a further reduction in EPE to 0.8068, suggesting that the complexity of the network can contribute to the

enhancement of stereo matching performance. Furthermore, we delve into the impact of pre-training on the MobileNetV2 100 backbone. Without pre-training, the EPE remains at 0.8227. However, when pre-trained, we observe a substantial improvement, as the EPE drops to 0.7132. This underscores the value of leveraging large-scale image datasets to enhance feature extraction capabilities before fine-tuning specific tasks like stereo matching. In conclusion, our ablation study highlights the critical role of both the architecture’s complexity and pre-training in refining the stereo matching model’s accuracy.

**Table 5:** Ablation study results of cost volume on the finalpass of SceneFlow test datasets [28]. For these experiments, one-quarter features from stereo images are utilized to construct the cost volume. Gwc represents Group-wise correlation volume [13]. Cat stands for Concatenation volume [5]. G8-C16, G16-C24 and G32-C48 combine Group-wise correlation volume and Concatenation volume [13]. Channel represents the channel of cost volume. Dims refers to the dimensions of cost volume.

| Cost Volume | Dims | Channel | Flops    | Params | EPE         |
|-------------|------|---------|----------|--------|-------------|
| Difference  | 3D   | -       | 17.44G   | 2.40M  | 1.02        |
| Correlation | 3D   | -       | 24.80G   | 4.01M  | 0.81        |
| Interlaced8 | 4D   | 8       | 126.87G  | 2.83M  | 0.70        |
| Gwc8        | 4D   | 8       | 31.83G   | 2.78M  | 0.71        |
| Gwc16       | 4D   | 16      | 75.28G   | 3.89M  | 0.66        |
| Gwc24       | 4D   | 24      | 147.53G  | 5.75M  | 0.63        |
| Gwc32       | 4D   | 32      | 248.60G  | 8.34M  | 0.62        |
| Gwc48       | 4D   | 48      | 537.15G  | 15.73M | <b>0.60</b> |
| Cat24       | 4D   | 24      | 148.36G  | 5.78M  | 0.65        |
| Cat48       | 4D   | 48      | 537.99G  | 15.76M | 0.61        |
| Cat64       | 4D   | 64      | 941.79G  | 26.09M | <b>0.60</b> |
| G8-C16      | 4D   | 24      | 148.36G  | 5.78M  | 0.62        |
| G16-C24     | 4D   | 40      | 379.30G  | 11.69M | <b>0.60</b> |
| G32-C48     | 4D   | 80      | 1460.80G | 39.37M | <b>0.60</b> |

**Cost Construction** In Table 5, an ablation study on various cost volume strategies for stereo matching is presented. The study begins with simpler 3D cost volume methods like Difference [21] and Correlation [46], yielding higher EPE of 1.02 and 0.81, respectively, at lower computational costs. This suggests that while efficient, these methods may lack the nuanced disparity capture necessary for complex scenes. The Interlaced8 model, introduced by MobileStereoNet [39], achieves the same EPE comparable to the Gwc8 model. However, its computational expense is substantially higher, with a flop count of 126.87G which is significantly larger than that of the Gwc8 model. The group-wise correlation and concatenation models demonstrate a clear trend: as the channel depth increases, the EPE improves, indicating improved disparity estimations through richer feature capture. The combined volume (G8-C16) offers a more optimal balance between computational load and disparity estimation accuracy, which achieves an EPE of 0.62. G16-C24 and G32-C48 do not result in significant improvement in EPE, which stabilizes at 0.60, despite a dramatic increase in computational load, especially for G32-C48 which demands 1460.80

Gflops and has 39.37M parameters. These results highlight the delicate balance between accuracy and computational efficiency in designing cost volumes for disparity estimation. While deeper and combined volumes reduce the EPE, the gains might be marginal compared to the significant increase in computational requirements, raising questions about the practicality of these approaches in resource-constrained environments.

**Table 6:** Ablation study results of disparity regression and refinement on the finalpass of SceneFlow test datasets [28]. ArgMin refers to Differentiable ArMin. Context stands for ContextUpasmp [25, 42, 51].

| Regression | Refinement               | Flops    | Params | EPE         |
|------------|--------------------------|----------|--------|-------------|
| ArgMin     | None                     | 26.37G   | 2.69M  | 0.76        |
| ArgMin     | RGBRefine [52]           | 53.15G   | 2.81M  | 0.72        |
| ArgMin     | Context                  | 31.83G   | 2.78M  | 0.71        |
| ArgMin     | Context+RGBRefine [52]   | 58.61G   | 2.89M  | 0.69        |
| ArgMin     | Context+DRNetRefine [52] | 58.57G   | 2.89M  | 0.69        |
| ArgMin     | ConvGRU [25, 51]         | 1363.71G | 12.51M | <b>0.46</b> |

**Disparity Regression and Refinement** The Differentiable ArgMin [5, 12, 13, 20, 39, 40, 46, 50, 58] introduced by GCNet [20], calculates initial disparity by converting matching costs into probabilities via softmax and then computing a weighted sum of these probabilities across all disparity levels. As shown in Table 6, in this ablation study on disparity refinement for the SceneFlow test datasets, various strategies show differing impacts on model performance. Without refinement, the model has an EPE of 0.76. RGBRefine and Context methods slightly improve EPE to 0.72 and 0.71, respectively, with a modest increase in computational resources. Combining these methods further reduces EPE to 0.69, indicating marginal benefits from their integration. However, employing ConvGRU refinement leads to a substantial improvement, reducing EPE to 0.46, albeit at a significant cost in computational complexity (1363.71 Gflops) and model size (12.51M). This highlights a trade-off between accuracy improvements and increased computational demands.

### 4.3 Analysis and Discussion

**Necessity of Comprehensive Ablation Study** In the evolving landscape of deep stereo matching, comprehensive ablation studies play a pivotal role in deciphering the effectiveness of different components and strategies. A thorough ablation study goes beyond mere performance metrics; it uncovers the underlying mechanics of different algorithms, revealing their strengths and weaknesses in various scenarios. For instance, different data augmentation techniques may yield contrasting effects on the model’s ability to match stereo images accurately. Similarly, the impact of varying backbones, cost volume configurations, and disparity regression methods on the overall performance can be profound.

Understanding the specific contributions of each component is crucial for building more efficient and effective stereo matching systems.

**Necessity of A Strong Baseline** A strong baseline in deep stereo matching research is critical for several key reasons. First, it serves as a vital reference point, enabling a clear assessment of new methods against an established standard. Second, a strong baseline allows for precise evaluation of the impact of specific changes, whether they are new data augmentation methods, different network architectures, or innovative disparity estimation techniques. This helps in isolating and understanding the contribution of each component to the overall performance. Additionally, a solid baseline ensures fair and meaningful comparisons across studies, providing a common ground for evaluating different research outcomes. This is crucial for maintaining consistency and validity in comparative analyses. In summary, a strong baseline is essential for meaningful advancements in deep stereo matching, ensuring that new developments are substantial, accurately assessed, and broadly applicable.

## 5 A Strong Pipeline: StereoBase

In light of our comprehensive analysis, the goal of this section is to establish a strong baseline model that surpasses existing standards in performance. StereoBase, our proposed solution, embodies this objective.

### 5.1 Pipeline

We build a strong baseline: StereoBase. StereoBase begins with a carefully curated data preprocessing step. For SceneFlow, KITTI2012, and KITTI2015, we implement an optimized mix of data augmentation techniques, including RandomCrop, ColorAug, and Erase Transform. This step ensures that the input data is not only varied and representative of real-world scenarios but also tailored to enhance stereo matching performance. Given the left and the right images, the pre-trained MobileNetV2 [48] networks are used as our foundational backbone, extracting features at a reduced scale of 1/4th the original size to form the cost volume. The cost volume utilizes a combined volume, which combines group-wise correlation volume with an 8-channel and concatenation volume with 16 channels, to ensure an optimal balance between computational load and disparity estimation accuracy. Hourglass networks [51] were implemented for cost aggregation, while convGRU [51] strategies were applied for the final disparity regression.

### 5.2 Comparison with State-of-the-art

In our comprehensive evaluation, we benchmarked StereoBase against current state-of-the-art methods on SceneFlow, KITTI2012, 2015, and DrivingStereo. On

**Table 7:** Results on SceneFlow [28], KITTI 2012 [11], KITTI 2015 [29] leaderboard, and DrivingStereo [55]. All results on DrivingStereo [55] are derived using the Open-Stereo. Underline refers to evaluation in the non-occluded regions only. **Bold:** Best.

| Method               | SceneFlow   |             | KITTI 2012  |             | KITTI 2015  |             |             | DrivingStereo |  |
|----------------------|-------------|-------------|-------------|-------------|-------------|-------------|-------------|---------------|--|
|                      | EPE         | 3-noc       | 3-all       | D1-bg       | D1-fg       | D1-all      | EPE         | D1-all        |  |
| STTR [24]            | <b>0.43</b> | -           | -           | 1.70        | 3.61        | 2.01        | OOM         | OOM           |  |
| CFNet [40]           | 1.04        | 1.23        | 1.58        | 1.54        | 3.56        | 1.88        | <b>0.98</b> | 1.46          |  |
| AANet [52]           | 0.87        | 1.91        | 2.42        | 1.65        | 3.96        | 2.03        | 2.91        | 15.16         |  |
| COEX [1]             | 0.68        | 1.55        | 1.93        | 1.74        | 3.41        | 2.02        | 1.34        | 2.70          |  |
| FADNet++ [46]        | 0.76        | -           | -           | 1.99        | 3.18        | 2.19        | 1.44        | 5.15          |  |
| PSMNet [5]           | 1.09        | 1.49        | 1.89        | 1.86        | 4.62        | 2.32        | 1.19        | 2.26          |  |
| GwcNet [13]          | 0.76        | 1.32        | 1.70        | 1.74        | 3.93        | 2.11        | 0.99        | <b>1.36</b>   |  |
| Mobilestereo-3D [39] | 0.80        | -           | -           | 1.75        | 3.87        | 2.10        | 1.06        | 1.61          |  |
| CascadeStereo [12]   | 0.72        | -           | -           | 1.59        | 4.03        | 2.00        | 1.31        | 2.84          |  |
| IGEV-Stereo [51]     | 0.47        | 1.12        | 1.44        | 1.38        | 2.67        | 1.59        | 1.06        | 1.50          |  |
| StereoBase(Ours)     | <b>0.34</b> | <b>1.00</b> | <b>1.26</b> | <b>1.28</b> | <b>2.26</b> | <b>1.44</b> | 1.15        | 2.19          |  |

the SceneFlow test set, we achieve a new SOTA EPE of 0.34. The quantitative comparisons, as summarized in Table 7, clearly illustrate the edge of StereoBase in handling complex stereo matching scenarios with greater precision. Further, we submitted our results to the KITTI2012 and 2015 leaderboard, where StereoBase outperformed all published methods across all metrics. On KITTI2015, our StereoBase outperforms IGEV [51] by 9.43% on D1-all metric, respectively. In addition, we evaluate the generalization performance of StereoBase. As shown in Table 8, StereoBase exhibited exceptional performance in a zero-shot setting, achieving state-of-the-art results. This evaluation further validates the adaptability and potential of StereoBase in handling diverse and challenging stereo vision tasks.

**Table 8:** Cross-domain evaluation on Middlebury, ETH3D, and KITTI all training sets. All methods are only trained on the Scene Flow datatest. Middlebury is tested on half-resolution. The model with  $\dagger$  indicates the implementation of OpenStereo. **Bold:** Best.

| Method                     | KITTI2012   |             | KITTI2015   |             | Middlebury  | ETH3D       |
|----------------------------|-------------|-------------|-------------|-------------|-------------|-------------|
|                            | D1-all(%)   | EPE         | D1-all(%)   | EPE         | bad 2.0(%)  | bad 1.0(%)  |
| STTR $^\dagger$            | 49.72       | 6.80        | 40.26       | 6.16        | OOM         | 38.89       |
| PSMNet $^\dagger$          | 30.51       | 4.68        | 32.15       | 5.99        | 33.53       | 18.02       |
| CFNet $^\dagger$           | 13.64       | 2.27        | 12.09       | 2.89        | 23.91       | 7.67        |
| AANet $^\dagger$           | 7.23        | 1.27        | 7.72        | 1.41        | 22.45       | 18.77       |
| Mobilestereo-2D $^\dagger$ | 18.34       | 2.45        | 21.21       | 2.78        | 34.04       | 13.89       |
| Mobilestereo-3D $^\dagger$ | 18.96       | 2.79        | 19.69       | 3.40        | 29.32       | 13.71       |
| GwcNet $^\dagger$          | 23.05       | 2.76        | 25.19       | 3.58        | 29.87       | 14.54       |
| COEX $^\dagger$            | 12.08       | 1.80        | 11.00       | 2.48        | 25.17       | 11.43       |
| FADNet++ $^\dagger$        | 11.31       | 1.77        | 13.23       | 2.97        | 24.17       | 25.53       |
| CascadeStereo $^\dagger$   | 11.83       | 1.83        | 12.03       | 2.69        | 27.27       | 11.68       |
| IGEV $^\dagger$            | 7.80        | 1.40        | 6.35        | 1.31        | 10.51       | 4.44        |
| StereoBase $^\dagger$      | <b>4.85</b> | <b>0.99</b> | <b>5.35</b> | <b>1.18</b> | <b>9.76</b> | <b>3.12</b> |

## 6 Conclusion

This paper introduces OpenStereo, a codebase designed for deep stereo matching. Our initial endeavor involved the re-implementation of the most state-of-the-art methods within the OpenStereo framework. This comprehensive tool facilitates the extensive reevaluation of various aspects of stereo matching methodologies. Drawing on the insights gained from our exhaustive ablation studies, we proposed StereoBase. StereoBase not only demonstrates the capabilities of our platform but also sets a new standard in the field for future research and development. Through OpenStereo and StereoBase, we aim to contribute a substantial and versatile resource to the stereo matching community, fostering innovation and facilitating more effective and efficient research.

## References

1. Antyanta Bangunharcana, Jae Won Cho, Seokju Lee, In So Kweon, Kyung-Soo Kim, and Soohyun Kim. Correlate-and-excite: Real-time stereo matching via guided cost volume excitation. In *IROS*, 2021.
2. Stan Birchfield and Carlo Tomasi. A pixel dissimilarity measure that is insensitive to image sampling. *TPAMI*, 1999.
3. Han Cai, Chuang Gan, Tianzhe Wang, Zhekai Zhang, and Song Han. Once for all: Train one network and specialize it for efficient deployment. In *ICLR*, 2020.
4. Z. Cao, G. Hidalgo Martinez, T. Simon, S. Wei, and Y. A. Sheikh. Openpose: Realtime multi-person 2d pose estimation using part affinity fields. *TPAMI*, 2019.
5. Jia-Ren Chang and Yong-Sheng Chen. Pyramid stereo matching network. In *CVPR*, 2018.
6. Kai Chen, Jiaqi Wang, Jiangmiao Pang, Yuhang Cao, Yu Xiong, Xiaoxiao Li, Shuyang Sun, Wansen Feng, Ziwei Liu, Jiarui Xu, Zheng Zhang, Dazhi Cheng, Chenchen Zhu, Tianheng Cheng, Qijie Zhao, Buyu Li, Xin Lu, Rui Zhu, Yue Wu, Jifeng Dai, Jingdong Wang, Jianping Shi, Wanli Ouyang, Chen Change Loy, and Dahua Lin. MMDetection: Open mmlab detection toolbox and benchmark. *arXiv preprint arXiv:1906.07155*, 2019.
7. Xuelian Cheng, Yiran Zhong, Mehrtash Harandi, Yuchao Dai, Xiaojun Chang, Hongdong Li, Tom Drummond, and Zongyuan Ge. Hierarchical neural architecture search for deep stereo matching. In *NeurIPS*, 2020.
8. Alexey Dosovitskiy, Philipp Fischer, Eddy Ilg, Philip Hausser, Caner Hazirbas, Vladimir Golkov, Patrick van der Smagt, Daniel Cremers, and Thomas Brox. Flownet: Learning optical flow with convolutional networks. In *ICCV*, 2015.
9. Shivam Duggal, Shenlong Wang, Wei-Chiu Ma, Rui Hu, and Raquel Urtasun. Deeppruner: Learning efficient stereo matching via differentiable patchmatch. In *ICCV*, 2019.
10. Chao Fan, Junhao Liang, Chuanfu Shen, Saihui Hou, Yongzhen Huang, and Shiqi Yu. Opengait: Revisiting gait recognition toward better practicality. In *CVPR*, 2023.
11. Andreas Geiger, Philip Lenz, and Raquel Urtasun. Are we ready for autonomous driving? the kitti vision benchmark suite. In *CVPR*, 2012.
12. Xiaodong Gu, Zhiwen Fan, Siyu Zhu, Zuozhuo Dai, Feitong Tan, and Ping Tan. Cascade cost volume for high-resolution multi-view stereo and stereo matching. In *CVPR*, 2020.

13. Xiaoyang Guo, Kai Yang, Wukui Yang, Xiaogang Wang, and Hongsheng Li. Group-wise correlation stereo network. In *CVPR*, 2019.
14. Kaiming He, Xiangyu Zhang, Shaoqing Ren, and Jian Sun. Deep residual learning for image recognition. In *CVPR*, 2016.
15. Xin He, Kaiyong Zhao, and Xiaowen Chu. Automl: A survey of the state-of-the-art. *arXiv preprint arXiv:1908.00709*, 2019.
16. Heiko Hirschmuller. Stereo processing by semiglobal matching and mutual information. *TPAMI*, 2007.
17. Eddy Ilg, Nikolaus Mayer, Tonmoy Saikia, Margret Keuper, Alexey Dosovitskiy, and Thomas Brox. Flownet 2.0: Evolution of optical flow estimation with deep networks. In *CVPR*, 2017.
18. Eddy Ilg, Tonmoy Saikia, Margret Keuper, and Thomas Brox. Occlusions, motion and depth boundaries with a generic network for disparity, optical flow or scene flow estimation. In *ECCV*, 2018.
19. Alex Kendall, Hayk Martirosyan, Saumitro Dasgupta, Peter Henry, Ryan Kennedy, Abraham Bachrach, and Adam Bry. End-to-end learning of geometry and context for deep stereo regression. In *ICCV*, 2017.
20. Alex Kendall, Hayk Martirosyan, Saumitro Dasgupta, Peter Henry, Ryan Kennedy, Abraham Bachrach, and Adam Bry. End-to-end learning of geometry and context for deep stereo regression. In *ICCV*, 2017.
21. Sameh Khamis, Sean Fanello, Christoph Rhemann, Adarsh Kowdle, Julien Valentin, and Shahram Izadi. Stereonet: Guided hierarchical refinement for real-time edge-aware depth prediction. In *ECCV*, 2018.
22. Jiankun Li, Peisen Wang, Pengfei Xiong, Tao Cai, Ziwei Yan, Lei Yang, Jiangyu Liu, Haoqiang Fan, and Shuaicheng Liu. Practical stereo matching via cascaded recurrent network with adaptive correlation. In *CVPR*, 2022.
23. Rui Li and Xiaolin Wu. Efficient dense stereo matching using adaptive window and census transform. *TIP*, 2013.
24. Zhaoshuo Li, Xingtong Liu, Nathan Drenkow, Andy Ding, Francis X. Creighton, Russell H. Taylor, and Mathias Uebert. Revisiting stereo depth estimation from a sequence-to-sequence perspective with transformers. In *ICCV*, 2021.
25. Lahav Lipson, Zachary Teed, and Jia Deng. Raft-stereo: Multilevel recurrent field transforms for stereo matching. In *3DV*, 2021.
26. Biyang Liu, Huimin Yu, and Yangqi Long. Local similarity pattern and cost self-reassembling for deep stereo matching networks. In *AAAI*, 2022.
27. Hanxiao Liu, Karen Simonyan, and Yiming Yang. Darts: Differentiable architecture search. In *ICLR*, 2018.
28. Nikolaus Mayer, Eddy Ilg, Philip Hausser, Philipp Fischer, Daniel Cremers, Alexey Dosovitskiy, and Thomas Brox. A large dataset to train convolutional networks for disparity, optical flow, and scene flow estimation. In *CVPR*, 2016.
29. Moritz Menze and Andreas Geiger. Object scene flow for autonomous vehicles. In *CVPR*, 2015.
30. Raúl Mur-Artal and Juan D. Tardós. Orb-slam2: An open-source slam system for monocular, stereo, and rgbd cameras. *IEEE Transactions on Robotics*, 2017.
31. Guang-Yu Nie, Ming-Ming Cheng, Yun Liu, Zhengfa Liang, Deng-Ping Fan, Yue Liu, and Yongtian Wang. Multi-level context ultra-aggregation for stereo matching. In *CVPR*, 2019.
32. Adam Paszke, Sam Gross, Francisco Massa, Adam Lerer, James Bradbury, Gregory Chanan, Trevor Killeen, Zeming Lin, Natalia Gimelshein, Luca Antiga, et al. Pytorch: An imperative style, high-performance deep learning library. *NeurIPS*, 2019.

33. Peter Pinggera, Thomas Pock, and Horst Bischof. Efficient graph-based segmentation for stereo matching. *IJCV*, 2015.
34. Matteo Poggi, Davide Pallotti, Fabio Tosi, and Stefano Mattoccia. Guided stereo matching. In *CVPR*, 2019.
35. Tonmoy Saikia, Yassine Marrakchi, Arber Zela, Frank Hutter, and Thomas Brox. Autodispnet: Improving disparity estimation with automl. In *ICCV*, 2019.
36. Daniel Scharstein, Heiko Hirschmüller, York Kitajima, Greg Krathwohl, Nera Nešić, Xi Wang, and Porter Westling. High-resolution stereo datasets with subpixel-accurate ground truth. In *GCPR*, 2014.
37. Daniel Scharstein and Richard Szeliski. A taxonomy and evaluation of dense two-frame stereo correspondence algorithms. *IJCV*, 2002.
38. Thomas Schops, Johannes L Schonberger, Silvano Galliani, Torsten Sattler, Konrad Schindler, Marc Pollefeys, and Andreas Geiger. A multi-view stereo benchmark with high-resolution images and multi-camera videos. In *CVPR*, 2017.
39. Faranak Shamsafar, Samuel Woerz, Rafia Rahim, and Andreas Zell. Mobilestereonet: Towards lightweight deep networks for stereo matching. In *WACV*, 2022.
40. Zhelun Shen, Yuchao Dai, and Zhibo Rao. Cfnet: Cascade and fused cost volume for robust stereo matching. *arXiv preprint arXiv:2104.04314*, 2021.
41. Xiao Song, Guorun Yang, Xinge Zhu, Hui Zhou, Zhe Wang, and Jianping Shi. Adastereo: A simple and efficient approach for adaptive stereo matching. In *CVPR*, 2021.
42. Zachary Teed and Jia Deng. Raft: Recurrent all-pairs field transforms for optical flow. In *Computer Vision–ECCV 2020: 16th European Conference, Glasgow, UK, August 23–28, 2020, Proceedings, Part II* 16, 2020.
43. Fabio Tosi, Yiyi Liao, Carolin Schmitt, and Andreas Geiger. Smd-nets: Stereo mixture density networks. In *CVPR*, 2021.
44. Hengli Wang, Rui Fan, Peide Cai, and Ming Liu. Pvstereo: Pyramid voting module for end-to-end self-supervised stereo matching. *ICRA*, 2021.
45. Qiang Wang, Shaohuai Shi, Shizhen Zheng, Kaiyong Zhao, and Xiaowen Chu. FADNet: A fast and accurate network for disparity estimation. In *ICRA*, 2020.
46. Qiang Wang, Shaohuai Shi, Shizhen Zheng, Kaiyong Zhao, and Xiaowen Chu. Fadnet++: Real-time and accurate disparity estimation with configurable networks. *arXiv preprint arXiv:2110.02582*, 2021.
47. Philippe Weinzaepfel, Thomas Lucas, Vincent Leroy, Yohann Cabon, Vaibhav Arora, Romain Brégier, Gabriela Csurka, Leonid Antsfeld, Boris Chidlovskii, and Jérôme Revaud. CroCo v2: Improved Cross-view Completion Pre-training for Stereo Matching and Optical Flow. In *ICCV*, 2023.
48. Ross Wightman. Pytorch image models. <https://github.com/rwightman/pytorch-image-models>, 2019.
49. Yuxin Wu, Alexander Kirillov, Francisco Massa, Wan-Yen Lo, and Ross Girshick. Detectron2. <https://github.com/facebookresearch/detectron2>, 2019.
50. Gangwei Xu, Junda Cheng, Peng Guo, and Xin Yang. Attention concatenation volume for accurate and efficient stereo matching. In *CVPR*, 2022.
51. Gangwei Xu, Xianqi Wang, Xiaohuan Ding, and Xin Yang. Iterative geometry encoding volume for stereo matching. In *CVPR*, 2023.
52. Haofei Xu and Juyong Zhang. Aanet: Adaptive aggregation network for efficient stereo matching. In *CVPR*, 2020.
53. Aimin Yang, Chunying Zhang, Yongjie Chen, Yunxi Zhuansun, and Huixiang Liu. Security and privacy of smart home systems based on the internet of things and stereo matching algorithms. *ISO4*, 2020.
54. Gengshan Yang, Joshua Manela, Michael Happold, and Deva Ramanan. Hierarchical deep stereo matching on high-resolution images. In *CVPR*, 2019.

55. Guorun Yang, Xiao Song, Chaoqin Huang, Zhidong Deng, Jianping Shi, and Bolei Zhou. Drivingstereo: A large-scale dataset for stereo matching in autonomous driving scenarios. In *CVPR*, 2019.
56. Qingxiong Yang, Liang Wang, Rui Gan, Minglun Gong, and Yunde Jia. Adaptive support-weight approach for correspondence search with outlier rejection. *TPAMI*, 2010.
57. Jure Zbontar, Yann LeCun, et al. Stereo matching by training a convolutional neural network to compare image patches. *Journal of Machine Learning Research*, 2016.
58. Feihu Zhang, Victor Prisacariu, Ruigang Yang, and Philip H.S. Torr. Ga-net: Guided aggregation net for end-to-end stereo matching. In *CVPR*, 2019.
59. Feihu Zhang, Xiaojuan Qi, Ruigang Yang, Victor Prisacariu, Benjamin Wah, and Philip Torr. Domain-invariant stereo matching networks. In *ECCV*, 2020.
60. Guoxuan Zhang, Jin Han Lee, Jongwoo Lim, and Il Hong Suh. Building a 3-d line-based map using stereo slam. *IEEE Transactions on Robotics*, 2015.
61. Jiawei Zhang, Xiang Wang, Xiao Bai, Chen Wang, Lei Huang, Yimin Chen, Lin Gu, Jun Zhou, Tatsuya Harada, and Edwin R Hancock. Revisiting domain generalized stereo matching networks from a feature consistency perspective. In *CVPR*, 2022.
62. Kai Zhang and Janusz Kosecka. Surface patch similarity for near-duplicate 3d model retrieval. *IJCV*, 2005.